Journal of Theoretical and Applied Information Technology
15th September 2025. Vol.103. No.17

ISSN: 1992-8645 www.jatit.org E-ISSN: 1817-3195

AUTOMATED DETECTION AND SEVERITY CLASSIFICATION OF KNEE OSTEOARTHRITIS USING A SCALABLE CONVOLUTIONAL NEURAL NETWORK

[1]RYAVADI BUCHA RAO, KASUKURTHI VENKATA RAO[2]

[1] Research Scholar, Andhra University College of Engineering, Department of CS&SE, Visakhapatnam, India

[2] Professor, Andhra University College of Engineering, Department of CS&SE, Visakhapatnam, India

[1]rpr0101@gmail.com, [2] professor_venkat@yahoo.com

ABSTRACT

Osteoarthritis of the knee is a common degenerative joint condition that lowers quality of life and causes disability, especially in people over 60. It is brought on by the knee joint's degenerating cartilage, which causes bone-on-bone contact, discomfort, stiffness, swelling, and restricted movement. Deep neural networks, specifically "CNNs (Convolutional Neural Networks)", have shown a lot of promise in medical image processing for the identification and classification of diseases. In order to categorize knee osteoarthritis utilizing X-ray pictures into five groups—Minimum, Healthy, Moderate, Doubtful, and Severe—this research presents SCSNet, a deep learning model. Precision, recall, F1 score, and accuracy had been employed to compare the model's performance to three pre-trained transfer learning models: "VGG-16", "ResNet-50", and "Xception". According to experimental results, SCSNet outperformed the transfer learning models in every metric assessed, achieving higher performance with 98% accuracy.

Keywords: *Knee Osteoarthritis, Deep Learning, Classification, Machine Learning, Scalable Convolutional Neural Network, VGG16.*

1. INTRODUCTION

The degenerative joint illness known as knee osteoarthritis is typified by the gradual loss of cartilage, which eventually results in the breakdown of bone. Pain, stiffness, edema, and limited joint movement are typical symptoms. Its development is impacted by a number of risk variables, including age, gender, race, inheritance, obesity, trauma, vitamin D insufficiency, and lifestyle. There are two types of disease, which evolves through several levels of severity:

- Primary knee osteoarthritis predominantly affects older individuals due to aging or genetic predisposition.
- Secondary knee osteoarthritis can develop earlier in life due to factors such as injuries, diabetes, obesity, sports activities, or rheumatoid arthritis.

A comparison of normal and osteoarthritic knee images is illustrated in Figure 1, highlighting the structural differences. A key symptom of knee osteoarthritis is joint stiffness, particularly in the morning or after prolonged inactivity, alongside pain and limited mobility. Current diagnostic approaches rely on clinical examinations, symptom assessments, and imaging techniques such as X-rays, MRI, and CT scans for evaluation.

Figure 1. Sample X-rays Knee Images. (a) Normal Knee Image (b) Osteoarthritis Knee Image

According to severity, knee osteoarthritis is categorized radiologically by employing the "Kellgren-Lawrence (KL)" grading system, which divides the condition into five different phases, from grade 0 to grade 4. Accurate grading of knee osteoarthritis is essential for determining disease progression and determining appropriate treatment strategies. The five KL grades are classified as subsequent: "Healthy (0)", "Doubtful (1)", "Minimal (2)", "Moderate (3)", and "Severe (4)". An illustration of the KL grading system is provided in Figure 2.

ISSN: 1992-8645 www.jatit.org E-ISSN: 1817-3195

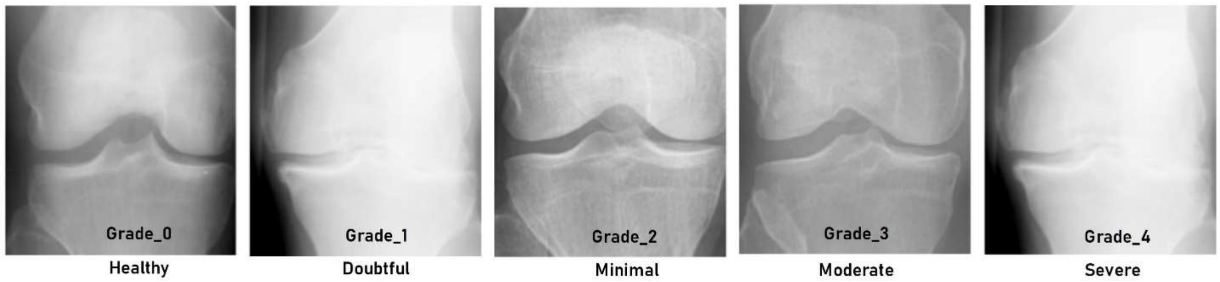

(a) (b) (c) (d) (e)

Figure.2. Sample image of dataset (a) Healthy (b) Doubtful (c) Minimal (d) Moderate and (e) Severe

1.1. Challenges

Palliative care is the cornerstone of treatment for osteoarthritis in the knee, for which there is presently no recognized cure. Because they provide thorough 3D imaging of knee joints, MRI and CT scans are useful diagnostic tools. The manual assessment of X-ray pictures, however, is costly and subject to expert subjectivity, which could result in inconsistent diagnoses. To minimize human errors, automated analysis of knee X-ray images using computer-assisted techniques is essential. Automation enhances diagnostic accuracy, reduces errors, and expedites the assessment process. Because knee osteoarthritis is classified using complicated criteria, orthopedic professionals need a lot of time to evaluate X-ray pictures. Early-stage osteoarthritis and structural distortions may obscure X-ray clarity, necessitating additional MRI scans. However, the high cost of MRI makes it less accessible for many patients. Traditional radiographic assessments often require highly skilled practitioners, multiple tests, and considerable time, leading to increased costs and potential inaccuracies. Current clinical diagnostic methods lack precision in effectively assessing osteoarthritis severity and progression. This study suggests a semi-automated method for diagnosing osteoarthritis in the knee in order to overcome these drawbacks. Using X-ray images, recent developments in Deep CNNs and ML have shown exceptional ability in identifying minute structural differences in knee joints. These techniques offer a more reliable, efficient, and cost-effective alternative to conventional diagnostic methods.

1.2. Motivation

Knee X-ray images typically lack prominent low-level structural details, making it challenging for deep CNNs to effectively learn classification patterns, especially when distinguishing between Kellgren-Lawrence (KL) grades, which often exhibit subtle differences. Many recent methods have directly applied existing image classification models without optimizing network architectures for the specific challenges of knee osteoarthritis diagnosis. While some approaches leverage architectural search techniques, most models were originally designed for generic image classification rather than medical imaging. Furthermore, state-of-the-art deep CNNs for knee osteoarthritis severity classification are often excessively large, exceeding 500 MB, requiring substantial computational resources that hinder real-time deployment. As a result, using well-known categorization models directly might not be the best option. Although recent approaches have started developing models tailored for knee osteoarthritis analysis, they still face limitations in accuracy and computational efficiency.

2. RELATED WORK

Deep learning (DL) approaches for knee osteoarthritis (KOA) classification have been widely explored. Jain et al. [15] utilized the High-Resolution Network (HRNet) to capture multi-scale features in knee X-rays, incorporating Gradient-based Class Activation Maps (Grad-CAMs) and an attention mechanism to enhance performance. However, the absence of complex features in some radiographs affected classification accuracy. Olsson et al. [16] employed a convolutional neural network (CNN) with the ResNet architecture, while Zhang et al. [17] implemented ResNet-18 and ResNet-34 for knee localization and KL-grade prediction. Yeoh, P. S. et al. [18] proposed a multitask deep learning model based on ResNet-34 to assess osteoarthritis severity and predict the likelihood of Total Knee Replacement (TKR) within nine years. Shamir et al. [19] introduced an approach that combined image descriptors, Fisher scores, and a weighted nearest neighbors' algorithm for KL-grade classification. Similarly, Guan et al. [20] integrated VGG16, DenseNet, and a Support Vector Machine (SVM) using non-image data for KOA prediction. For knee joint space width (JSW) localization, Abdullah and Rajasekaran [21] employed Faster Region-based CNN (RCNN), using AlexNet for severity classification and ResNet-50 for feature extraction.

ISSN: 1992-8645 www.jatit.org E-ISSN: 1817-3195

However, their patient selection criteria—focusing on individuals over 50 with OA symptoms could introduce bias and limit model generalizability. Tiulpin et al. [22] developed a Siamese network to learn similarity metrics between radiographs, while Cueva et al. [23] proposed a semi-automatic CADx model for KL-grade classification using Deep Siamese CNNs and ResNet-34. The reduction of image resolution to 8-bit in their study may have led to information loss, impacting accuracy. This study aims to develop a DL model for KOA classification using digitized knee X-ray images. Transfer learning techniques will be employed to adapt deep learning models to the KOA dataset, ensuring accurate detection and validation through comprehensive testing.

2.2. Our Contributions

The following are our additions, which are based on the shortcomings of best published works to date:

This work proposes an effective deep CNN model, SCSNet, for knee osteoarthritis severity prediction based on KL grades using X-ray images. Unlike conventional approaches that blindly apply pre-trained deep models, our method is specifically designed to account for the spatial scale of X-ray images, leading to more accurate and efficient classification. Finally, a comprehensive set of “tests and a Grad-CAM [20] visualization is presented to support the significance of every module in proposed framework. The remainder of the document is structured as follows: Related work is included in Section 2. The suggested approach is presented in Section 3. The” included dataset, training specifics, competing approaches, and evaluation measures are briefly described in Section 4. Experimental results and a brief explanation of the suggested scheme's learning in terms of Grad-CAM visualization of the obtained data are presented in Section 5, and Section 6 concludes the paper.

3. PROPOSED METHODS

The proposed work's flowchart is displayed in Figure 3. The pipeline initiates the X-ray equipment that takes patient X-rays and stores them in a database. The X-ray-generated images are utilized to train the categorization labeling model.

3.1. Data Augmentation

A significant problem in machine learning is “overfitting, which happens when a model learns a function with an abnormally high variance. This results in almost flawless performance on training data but poor generalization to new data”. By using altered versions of preexisting photos to artificially enlarge the training dataset, data augmentation is a useful strategy to reduce overfitting. Models trained on bigger and more varied datasets tend to be more accurate in deep learning, while augmentation approaches improve the models' capacity to generalize to new data. To add variations to the dataset, image data augmentation entails a variety of changes, including normalization, rotation, shifts, flips, and brightness alterations. Real-time data augmentation had been performed in this research by employing the Keras Image Data Generator, which ensures that the model receives fresh image changes at every training epoch, enhancing generalization and minimizing overfitting.

3.2. Image Scaling

Pixel values in the majority of image collections are expressed as integers between 0 and 255. However, when working with huge integer values, neural networks—procedure inputs with relatively modest weight values—may encounter learning that is slowed down or interrupted. Image normalization is therefore a common procedure to improve stability and computational efficiency. The process of normalization entails dividing all pixel values by a maximum value of 255 in order to scale them to a range between 0 and 1. This procedure is conducted consistently over all channels, regardless of the initial pixel value distribution of the image. The process of normalizing images improves the stability of the gradient descent algorithm, speeds up convergence, and increases numerical stability. The picture Data Generator technique was used in this study to accomplish picture normalization, with rescale=1./255 as its argument. This ensured that the neural network performed at its best throughout training.

3.3. Image Resizing

In computer vision, resizing images is a crucial first step that improves computational efficiency and ensures consistency. Machine learning algorithms typically train faster on smaller images, as larger images contain more pixels, thereby increasing the computational complexity. Furthermore, while raw photos frequently change in size, deep learning models require consistent input dimensions. The dataset used in this study included images of different resolutions, which can have a detrimental effect on the network's accuracy. To address this disparity, each image was scaled to a consistent 224 by 224 pixel size using OpenCV. This approach not only aligns with the input requirements of pre-trained models but also optimizes training efficiency by reducing computational demands while preserving essential image features.

3.4. Model Training

The “dataset is separated into training and validation sets after the images are preprocessed to ensure model compatibility for training. A cosine similarity

ISSN: 1992-8645 www.jatit.org E-ISSN: 1817-3195

layer, max-pooling layer, flattened layer, and dense layer are among the layers that make up the SCS-Net architecture. The SCS-Net model's structure, which integrates these layers, is shown in Figure 4. The

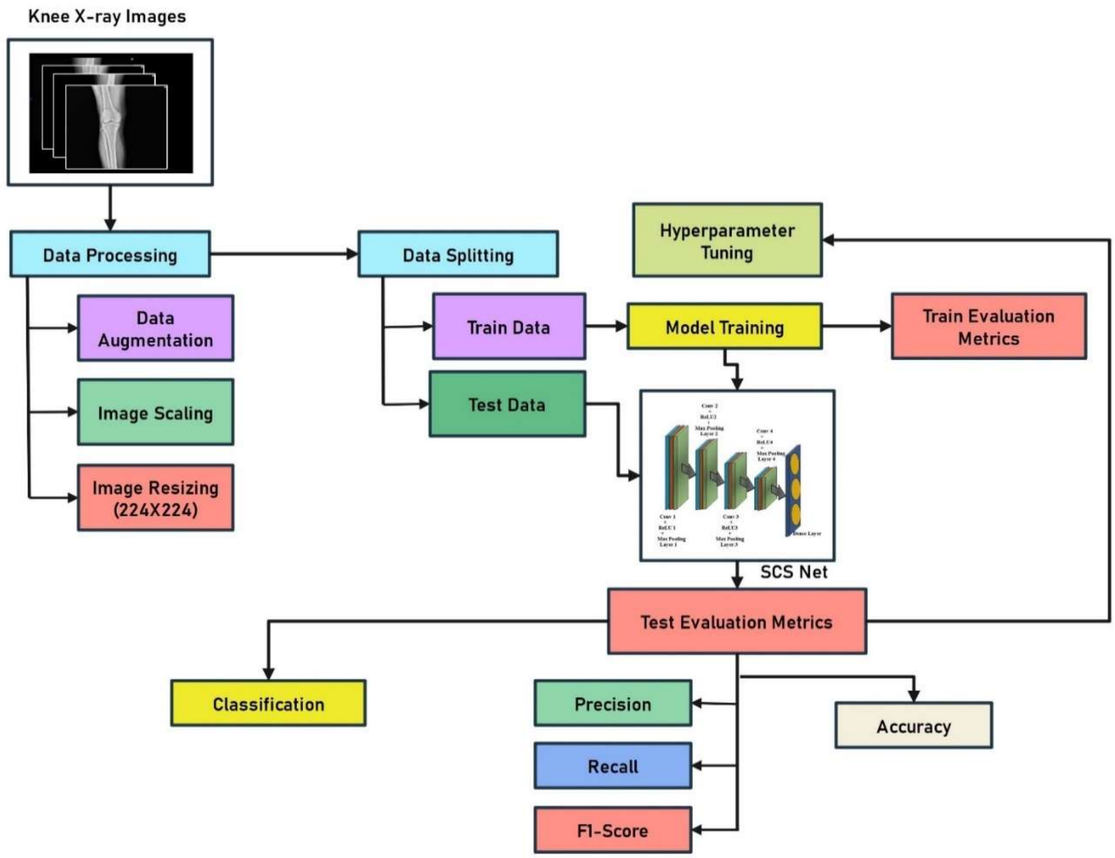

Figure.3. Block diagram representation of the proposed work for the diagnosis of osteoporosis.

validation set is used for evaluation using performance metrics that involve accuracy, precision, recall, F1-score, and Cohen's kappa score", whereas the training set is used to build the model. Furthermore, a comparison of the model's accuracy across several cutting-edge architectures is made. An alternate method for feature extraction in neural networks is provided by the SCS layer, which creates the feature map in contrast to traditional convolutional layers. SCS uses a stride technique to extract features from an image, just like convolution does. Nevertheless, it normalizes the kernel and the image patch to a unit magnitude prior to executing the operation, producing a cosine similarity measure, often referred to as cosine normalization, rather than directly computing the dot product [21].

$$\cos(\theta) = \frac{X.Y}{\|X\|\|Y\|} \tag{1}$$

$$SCD(X,Y) = \left(\frac{X.Y}{\left(\|X\|+Q\right)\left(\|Y\|+Q\right)} \right)^{p} \tag{2}$$

$$SCD(X,Y) = \mathrm{sign}(X.Y)\left(\frac{X.Y}{\left(\|X\|+Q\right)\left(\|Y\|+Q\right)} \right)^{p} \tag{3}$$

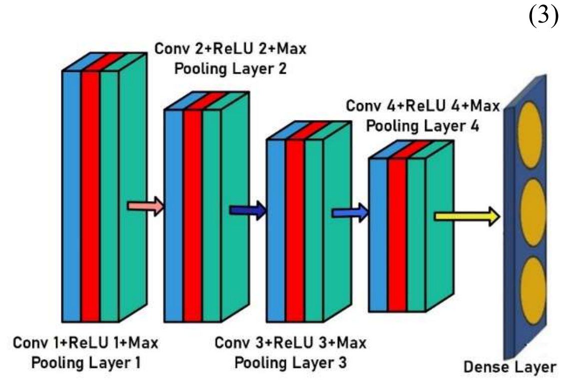

Figure.4. Architecture of "SCS-Net

ISSN: 1992-8645 www.jatit.org E-ISSN: 1817-3195

here, X=*Input* , Y=*Kernel* , Q=*Scale invariance* , P = *Sharpening Exponents* . SCS and other convolution-like" stride processes take features out of pictures. Equations (2) and (3) provide mathematical formulations for the Sharpened Cosine Distance (SCD) and Sharpened Cosine Similarity (SCS), respectively. Peak sharpening can be improved by raising it to an exponent, but each unit's sharpening exponents must be learned separately [22]. This method eliminates the need for normalization or activation functions after SCS layers and outperforms traditional convolutional neural networks while using 10x to 100x fewer parameters. However, cosine similarity is broad, so even dissimilar vectors might be similar. Sharpening fixes this by retaining the sign but boosting the result's power. Numerical instability may occur when the signal or kernel magnitude becomes close to zero. This is avoided by modestly raising the input strength to avoid the kernel magnitude becoming too narrow. Due to the ineffective parallelization of exponentiation processes, SCS's computational inefficiency on GPUs and TPUs is a major drawback. Although parameter reduction greatly improves GPU performance, the sharpening effect of SCS is also compromised.

3.5. Absolute Max-Pooling, Flatten, and Dense Layer

A dimensionality reduction method called pooling down samples while keeping important characteristics. This procedure extracts the most important information from feature maps, improving computing efficiency and lowering overfitting. During training, the pooling filter is iteratively refined through backpropagation until an optimal value is achieved for feature extraction in specific images. Max pooling, a widely used pooling technique, selects the highest magnitude value within a defined window, regardless of whether the element is positive or negative. The mathematical formulation for "max pooling is provided in Equation(4).

$$\textit{Abs Max Pooling} = \left| \left(\left(\mathbf{N} + \mathbf{2P} - -\frac{\mathbf{F}}{\mathbf{S}} \right) + \mathbf{1} \right) \right| \quad (4)$$

where, N = *Image Size* , P = *Size of Padding* , F = *Size of Filter* , S = *Stride* .

In order to facilitate smooth input into the Dense Layer for additional processing, the Flatten Layer converts multidimensional input data into a one-dimensional column vector". The completely linked neurons that make up the Dense Layer make it easier to memorize intricate patterns. Whereas the "Sigmoid activation function" is utilized for binary classification to produce probabilities for two different categories, the "SoftMax activation function" is utilized for multiclass classification to produce probability distributions over multiple classes.

3.6. Model Parameter Tuning

A batch size of 64, 40 epochs, and a learning rate of 0.0001 have been employed to train the SCS-Net model. A combination of momentum and RMSprop optimizers are used to improve the model; the Adam optimizer was chosen due to its low memory consumption and computational efficiency. To improve the robustness of the suggested model, hyperparameters are adjusted using the Keras tuner package. By choosing the step size for minimizing the loss function, the learning rate affects how quickly the model converges. Momentum preserves parameter update directionality, speeding convergence and improving accuracy. SoftMax activation has been employed for multiclass classification in the output layer, while sigmoid activation is employed for binary classification.

3.7. K-Fold Cross Validation

One method for preventing overfitting in a prediction model is cross-validation, which is particularly helpful when there is a limited quantity of data available. "A value for cross-validation is chosen, and the dataset is divided into equal-sized partitions. After splitting, partitions are employed for training and one for testing. This approach is done times, every time, using a different partition for testing. In this" investigation, 5-fold cross-validation is used.

3.8. Evaluation Metrics

Evaluation metrics provide for a methodical and impartial "assessment of a model's efficacy by giving a numerical depiction of its performance. Accuracy, precision, recall, and F1-score have been employed to assess the model's performance. A" confusion matrix is also included for a thorough examination of classification results. To illustrate the effectiveness of the suggested model, it is contrasted with these metrics. Figure 5 shows the confusion matrix, which graphically depicts the predictive performance of model.

4. Experiments and Results

The dataset for knee osteoarthritis severity classification was obtained from Kaggle, an open-source platform. Figure 4 illustrates the training, testing, as well as validation split "of the X-ray dataset. The dataset comprises 8,381 images, categorized based on the severity of knee osteoarthritis". The training set contains 5,097

ISSN: 1992-8645 www.jatit.org E-ISSN: 1817-3195

images, with the following label distribution: 2,286 Minimal, 1,046 Healthy, 1,516 Moderate, 757 Doubtful, and 173 Severe**.** To forecast the severity of knee issues in fresh X-ray images, machine learning models are mostly trained using this collection. The testing set consists of 2,458 photos, of which 296 are healthy, 447 are moderate, 223 are doubtful, 51 are severe, and 639 are minimal. Models that have been trained on the training set are evaluated using this subset.

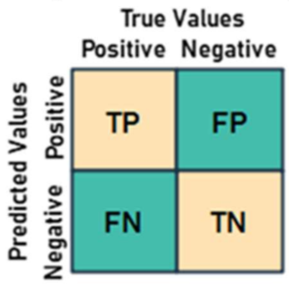

- True Positive (TP): True positive value be predicted to positive value.
- False Positive (FP): True positive value be predicted to negative value.
- True Negative (TN): True negative value be predicted to negative value.
- False Negative (FN): True negative value be predicted to positive value.

Figure.5. Confusion Matrix

- One crucial indicator is accuracy, which is the percentage of correct predictions the model made.

  Accuracy Score = (TP + TN)/ (TP + FN + TN + FP)
- Precision is a proportion of positive results that are true positives

  Precision Score = TP / (TP + FP)
- The Recall is a proportion of actual positives that were identified correctly

  Recall Score = TP / (TP +FN)
- F1-Score is a harmonic mean of precision and recall score

  F1 Score = 2* ((Precision Score * Recall Score) / (Precision Score + Recall Score))

Figure 6.Performance Metrics of the Proposed Model

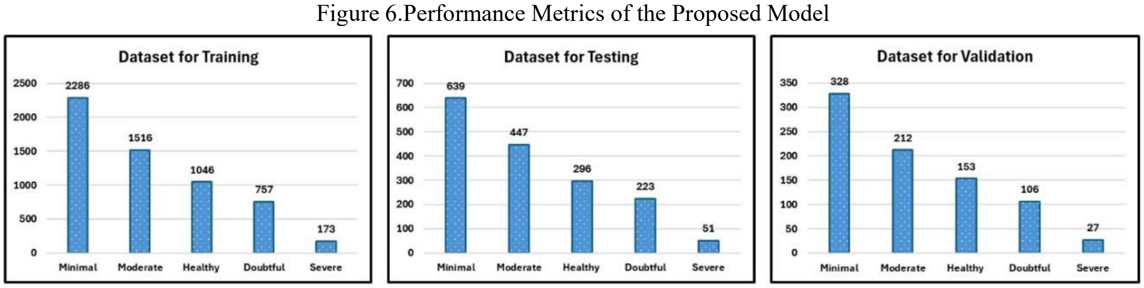

Figure.7. Dataset splitting (a) Training, (b) Testing, and (c) Validation

4.1. Analysis based on Confusion Matrix (CM)

A "confusion matrix evaluates a classification model's efficacy by comparing expected and actual values. It offers a more thorough and comprehensive view of the model's performance as opposed to depending solely on accuracy or other summary metrics. The confusion matrix obtained from three models is depicted in Figure 5. The CM for the VGG-16 model is depicted" in "Figure 8(a), the confusion matrix for the ResNet50 model is depicted in Figure 8(b), the confusion matrix for the Xception model is depicted in Figure 8(c), and the confusion matrix for the suggested CNN model is shown in Figure 8(d). This matrix shows true positive, true negative, false positive, and false negative. Accuracy, precision, recall, and F1-Score can be computed" using confusion matrix values. We suggest employing confusion matrices with other assessment metrics to evaluate a categorization model's efficacy more thoroughly and educationally. Figure 8 indicates that, in comparison to other transfer learning models, the "suggested CNN model's confusion matrix produces the best results. By contrasting expected and actual results, a

ISSN: 1992-8645 www.jatit.org E-ISSN: 1817-3195

confusion matrix offers a thorough assessment of a categorization model. In contrast to other summary measures like accuracy, it provides a thorough evaluation of the model's performance. Figure 8 shows comparisons: Figure 8(a) for VGG-16, Figure 8(b) for ResNet50, Figure 8(c) for Xception, and Figure 8(d) for the suggested CNN model. The confusion matrices from three models are displayed in Figure 5. For accuracy, precision, recall, and F1-score, the confusion matrix's" TP, TN, FP, and FN values are employed. Confusion matrices should be employed with other evaluation tools for a more complete and informative analysis. It is clear from Figure 8 that the suggested SCS-Net model performs better than the transfer learning models and produces the best classification outcomes.

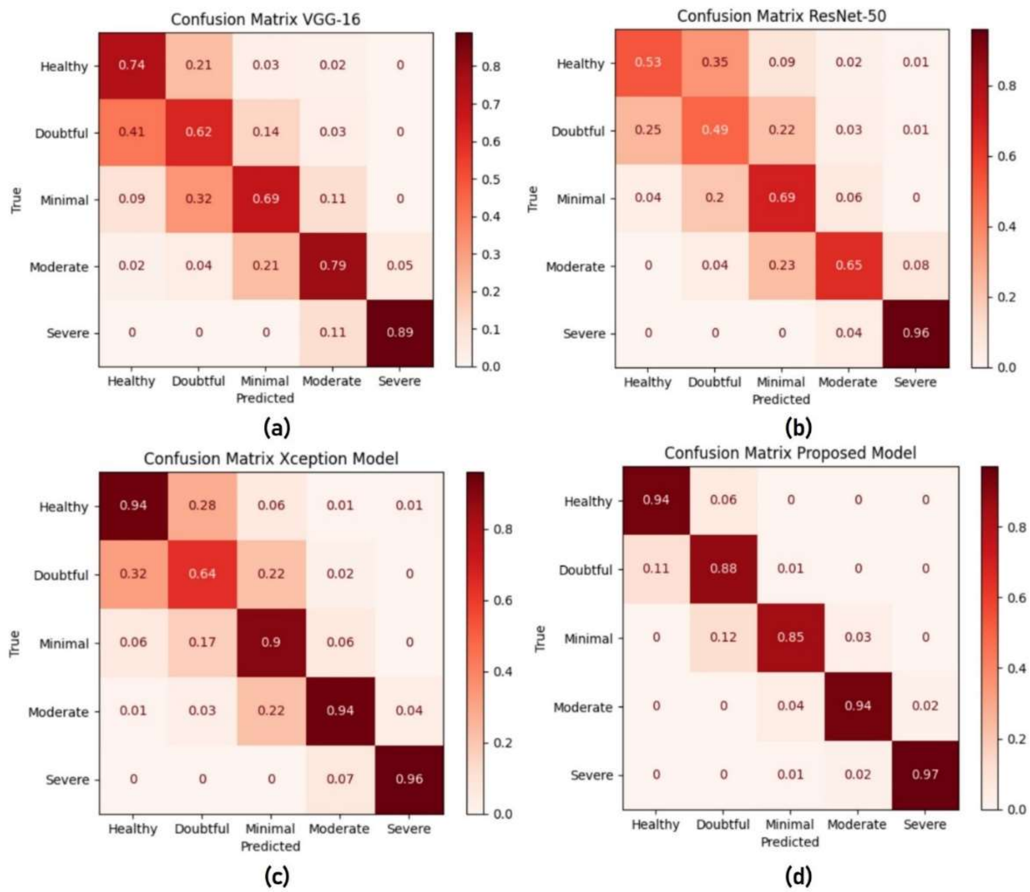

Figure.8. Confusion matrix (a) VGG-16 (b) ResNet-50 (c) Xception model (d) Proposed SCS-Net

4.2. Analysis based on accuracy plot

Accuracy and loss plots are crucial visualization tools in machine learning that are employed to determine a model's performance during training. Plotting accuracy (y-axis) versus training epochs, the accuracy plot shows how well the model can categorize input samples. The accuracy plot usually displays an upward trend as the model learns, indicating better classification performance. Similarly, the loss plot depicts how successfully the model minimizes differences between expected and actual values by tracking its mistake. The model's learning process, possible overfitting, and convergence behavior are all revealed by these visuals. The accuracy graphs for the four models are shown in Figure 9. The VGG-16 model's accuracy plot is depicted in Figure 9(a), followed by the ResNet50 model in Figure 9(b), the Xception model in Figure 9(c), and the suggested SCS-Net model in Figure 9(d). The training accuracy is shown by the blue line in each plot, while the validation accuracy is shown by the orange line. Better learning stability and generalization are indicated by the suggested SCS-Net model's smoother curves and greater accuracy values when compared to all other models.

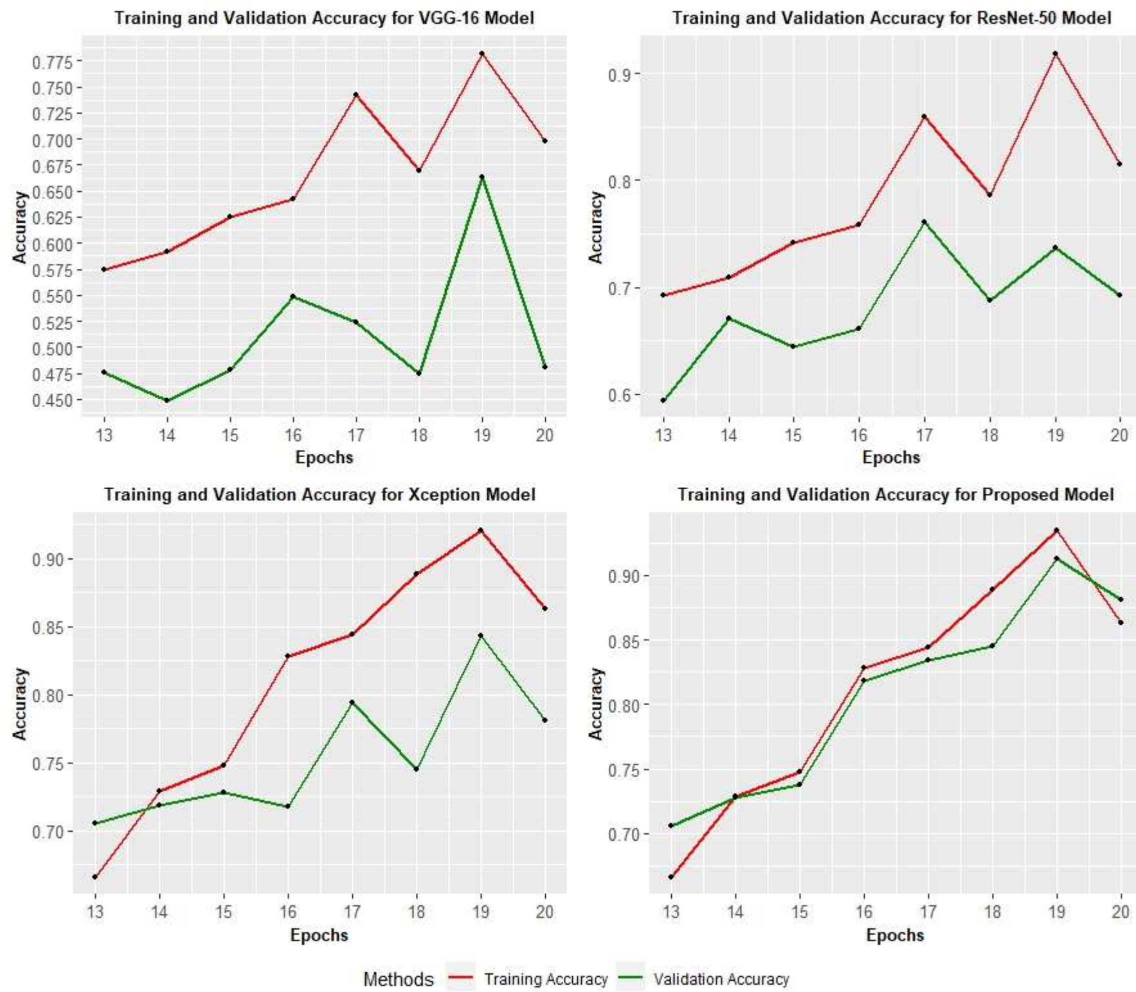

Figure.9. Accuracy plots (a) VGG-16 Model, (b) ResNet50 model, (c) Xception model and (c) Proposed CNN

4.3. Analysis based on performance parameters

In order to classify varying degrees of disease severity within a medical dataset, Figure 10 compares four machine learning models: VGG-16, ResNet50, Xception, and the suggested SCS-Net model. The five severity classes—Minimum, Healthy, Moderate, Doubtful, and Severe—are used to evaluate performance depending on "precision", "recall", "F1-score", and "accuracy". The findings show that the suggested model performs better than the other three models in every evaluation criteria, attaining the highest scores in every severity class. Notably, the SCS-Net model exhibits excellent classification performance by achieving perfect scores for the Severe category and maintaining "high precision, recall, and F1-score for the remaining classes. On the other hand, Xception displays poorer precision and F1 scores for the Moderate class, whereas ResNet50 displays lower recall and F1 scores for the Minimal, Healthy, and Moderate" classes. The efficiency of the suggested SCS-Net model is further supported by the fact that it exhibits shorter processing times than the transfer learning models. All things considered; these results point to the suggested SCS-Net model as the best option for precisely identifying illness severity levels. The findings show that the pre-trained suggested SCS-Net model outperformed the VGG-16, ResNet50, and Xception models in terms of training and testing accuracy. This demonstrates how well the suggested approach works with X-ray pictures for the early diagnosis of osteoarthritis in the knee. Prediction visualizations were produced for randomly chosen photos from the dataset to further verify the model's efficacy and demonstrate its capacity to correctly classify the severity of the condition. Furthermore, Grad-CAM visualization was used to make the X-ray pictures more interpretable by emphasizing the crucial areas that influenced the model's predictions. The accuracy and dependability of the model in identifying osteoarthritis in the knee are further supported by these visualizations, which are shown in Figure 11.

5. Conclusion

In this study, we developed the SCSNet model to use X-ray images to categorize the severity of osteoarthritis in the knee. It outperformed three pre-trained transfer learning models—VGG-16, ResNet-50, and Xception—with 98% accuracy, greatest precision, recall, and F1 score. These findings demonstrate how well SCSNet can detect and classify knee osteoarthritis into five different severity levels. Clinical applications of the suggested paradigm are highly promising, helping medical practitioners make accurate diagnoses and enhance patient care. Future studies might look into other improvements, such as incorporating multi-modal data or improving the model for clinical application in real-time.

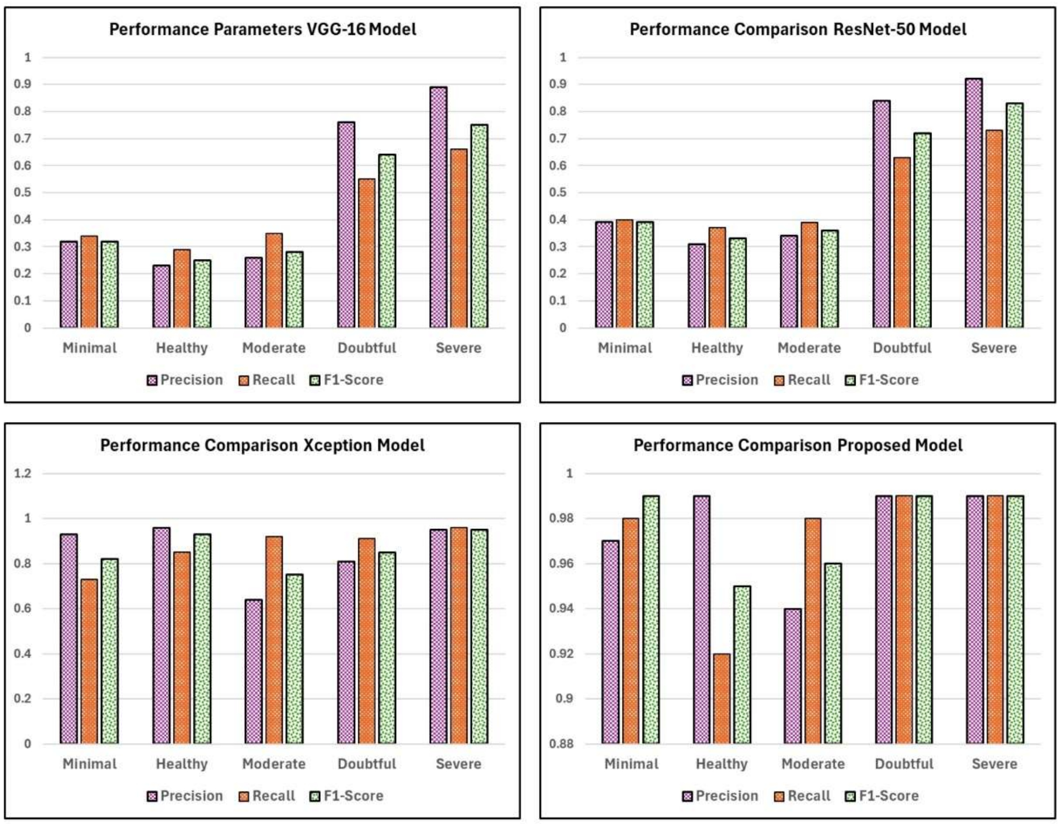

Figure.10. Performance Parameters Comparison

ISSN: 1992-8645 www.jatit.org E-ISSN: 1817-3195

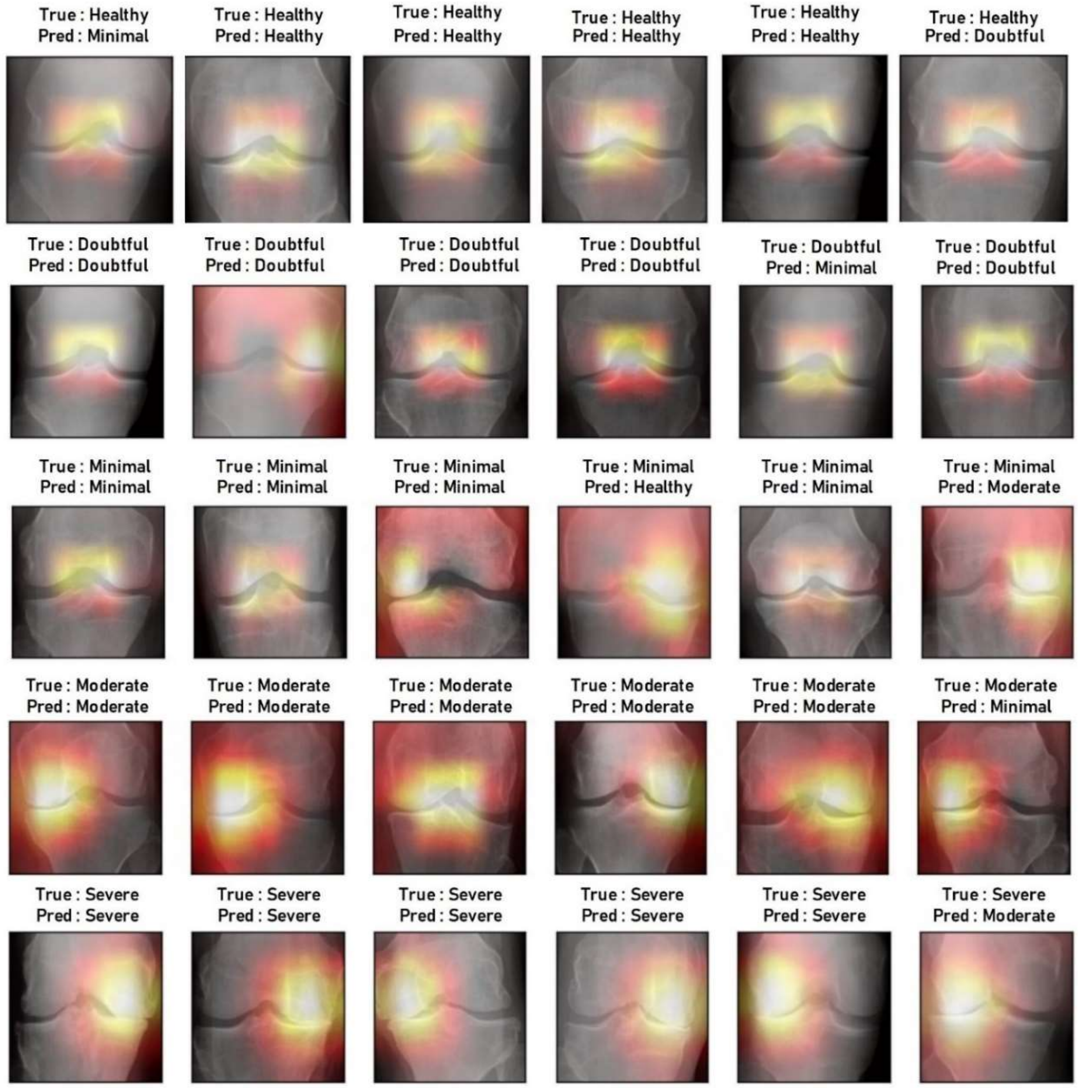

Figure.11. Predictions obtained with the proposed model on randomly selected X-ray images from the dataset.

REFERENCES:

[1] S. Oh, E. Jang, Y. Oh, W. Kang, E. Lee et al., "An exploratory study on the reliability of degenerative knee arthritis dialectics and the correlation between knee ROM, VAS, and WOMAC," Journal of Korean Medicine Rehabilitation, vol. 29, no. 3, pp. 113–128, 2019.

[2] J. Zhu, L. Sun, Y. Wang, S. Subramani, D. Peng et al., "A ResNet based multiscale feature extraction for classifying multi-variate medical time series," KSII Transactions on Internet and Information Systems, vol. 16, no. 5, pp. 1431–1445, 2022.

[3] X. Xu, J. Zhang, X. Cheng, L. Lu, Y. Zhao et al., "A tuberculosis detection method using attention and sparse R-CNN," KSII Transactions on Internet and Information Systems, vol. 16, no. 7, pp. 2131–2153, 2022.

[4] N. Bayramoglu, M. T. Nieminen and S. Saarakkala, "A lightweight CNN and joint shape-joint space (JS2) descriptor for radiological osteoarthritis detection," Medical Image Understanding and Analysis, vol. 1248, pp. 331–345, 2020.

[5] K. Lee and E. Kim, "Deep learning model lightweight technology analysis," Korea Institute of Science and Technology Information, pp. 1–89, 2020. https://doi.org/10.22648/ETRI.2019.J.340205.

[6] H. B. Baydargil, J. Park, D. Kang, H. Kang and K. Cho, "A parallel deep convolutional neural network for Alzheimer's disease classification on PET/CT brain images," KSII Transactions on

ISSN: 1992-8645 www.jatit.org E-ISSN: 1817-3195

Internet and Information Systems, vol. 14, no. 9, pp. 3583–3597, 2020.

[7] P. Chen, L. Gao, X. Shi, K. Allen and L. Yang, "Fully automatic knee osteoarthritis severity grading using deep neural networks with a novel ordinal loss," Computerized Medical Imaging and Graphics, vol. 75, no. 9, pp. 84–92, 2019.

[8] K. A. Thomas, Ł. Kidziński, E. Halilaj, S. L. Fleming, G. R. Venkataraman et al., "Automated classification of radiographic knee osteoarthritis severity using deep neural networks," Radiology: Artificial Intelligence, vol. 2, no. 22020. https://doi.org/10.1148/ryai.2020190065.

[9] R. K. Jain, P. K. Sharma, S. Gaj, A. Sur and P. Ghosh, "Knee osteoarthritis severity prediction using an attentive multi-scale deep convolutional neural network," arXiv preprint arXiv: 2106.14292, 2021.

[10] J. S. Yadav, S.S., "Deep convolutional neural network based medical image classification for disease diagnosis." J Big Data 6, 113, 2019.

[11] G. Huang, Z. Liu, L. van der Maaten, and K. Q. Weinberger, "Densely connected convolutional networks," 2018.

[12] . Wang, K. Sun, T. Cheng, B. Jiang, C. Deng, Y. Zhao, D. Liu, Y. Mu, M. Tan, X. Wang, W. Liu, and B. Xiao, "Deep high-resolution representation learning for visual recognition," IEEE Transactions on Pattern Analysis and Machine Intelligence, pp. 1–1, 2020.

[13] A. Paszke, S. Gross, F. Massa, A. Lerer, J. Bradbury, G. Chanan, T. Killeen, Z. Lin, N. Gimelshein, L. Antiga, A. Desmaison, A. Kopf, E. Yang, Z. DeVito, M. Raison, A. Tejani, S. Chilamkurthy, B. Steiner, L. Fang, J. Bai, and S. Chintala, "Pytorch: An imperative style, highperformance deep learning library," pp. 8024–8035, 2019.

[14] M. M. Fatihin, F. Baskoro, and L. Anifah, "Texture Analysis of Knee Osteoarthritis Using Contrast Limited Adaptive Histogram Equalization Based Gray Level Co-occurrent Matrix". In 2020 Third International Conference on Vocational Education and Electrical Engineering (ICVEE) (pp. 1-4). IEEE, 2020.

[15] Jain, R.K., Sharma, P.K., Gaj, S., Sur, A., Ghosh, P. (2021). Knee osteoarthritis severity prediction using an attentive multi-scale deep convolutional neural network. arXiv preprint arXiv:2106.14292. https://doi.org/10.48550/arXiv.2106.14292.

[16] Olsson, S., Akbarian, E., Lind, A., Razavian, A.S., Gordon, M. (2021). Automating classification of osteoarthritis according to Kellgren-Lawrence in the knee using deep learning in an unfiltered adult population. BMC Musculoskeletal Disorders, 22(1): 1-8. https://doi.org/10.1186/s12891-021-04722-7.

[17] Zhang, B., Tan, J., Cho, K., Chang, G., Deniz, C.M. (2020). Attention-based CNN for kl grade classification: Data from the osteoarthritis initiative. In 2020 IEEE 17th International Symposium on Biomedical Imaging (ISBI), Iowa City, IA, USA, pp. 731-735. https://doi.org/10.1109/ISBI45749.2020.9098456.

[18] Leung, K., Zhang, B., Tan, J., Shen, Y., Geras, K.J., Babb, J.S., Cho, K., Chang, G., Deniz, C.M. (2020). Prediction of total knee replacement and diagnosis of osteoarthritis by using deep learning on knee radiographs: Data from the osteoarthritis initiative. Radiology, 296(3): 584-593. https://doi.org/10.1148/radiol.2020192091.

[19] Shamir, L., Ling, S.M., Scott, W.W., Bos, A., Orlov, N., Macura, T.J., Eckley, D.M., Ferrucci, L., Goldberg, I.G. (2008). Knee x-ray image analysis method for automated detection of osteoarthritis. IEEE Transactions on Biomedical Engineering, 56(2): 407-415. https://doi.org/10.1109/TBME.2008.2006025.

[20] Guan, B., Liu, F., Mizaian, A.H., Demhri, S., Neogi, T., Guermazi, A., Kijowski, R. (2019). Deep learning approach to predict radiographic knee osteoarthritis progression. Osteoarthritis and Cartilage, 27: S395-S396. https://doi.org/10.1016/j.joca.2019.02.396.

[21] Abdullah, S.S., Rajasekaran, M.P. (2022). Automatic detection and classification of knee osteoarthritis using a Deep Learning approach. La Radiologia Medica, 127(4): 398-406. https://doi.org/10.1007/s11547-022-01476-7.

[22] Cueva, J.H., Castillo, D., Espinós-Morató, H., Durán, D., Díaz, P., Lakshminarayanan, V. (2022). Detection and classification of knee osteoarthritis. Diagnostics, 12(10): 2362. https://doi.org/10.3390/diagnostics12102362 .

[23] Tiulpin, A., Thevenot, J., Rahtu, E., Lehenkari, P., Saarakkala, S. (2018). Automatic knee osteoarthritis diagnosis from plain radiographs: A deep learning-based approach. Scientific Reports, 8(1): 1727. https://doi.org/10.1038/s41598-018-20132-7.

[24] Singh, S., Aggarwal, A.K., Ramesh, P., Nelson, L., Damodharan, P. and Pandian, M.T., 2022, August. COVID 19: Identification of Masked Face using CNN Architecture. In 2022 3rd International Conference on Electronics and Sustainable Communication Systems (ICESC)

(pp. 1045–1051). IEEE. https://doi.org/10.1109/ICESC54411.2022.9885327

[25] Sharma, N., Gupta, S., Mehta, P., Cheng, X., Shankar, A., Singh, P. and Nayak, S.R., 2022. Offline signature verification using deep neural network with application to computer vision. Journal of Electronic Imaging, 31(4), pp. 041210–041210. https://doi.org/10.1117/1.JEI.31.4.041210